iScience

CellPress
OPEN ACCESS

Article

Human CD4$^+$ memory phenotype T cells use mitochondrial metabolism to generate sensitive IFN-γ responses

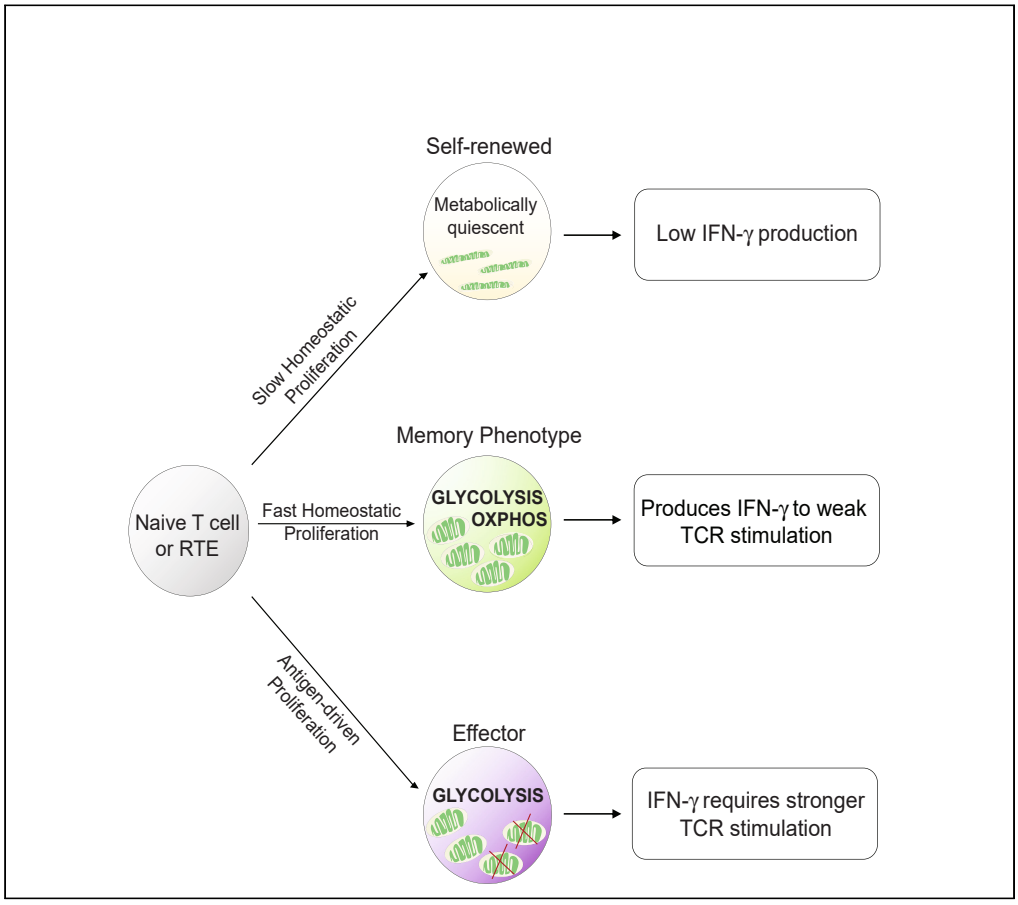

Nikhila S. Bharadwaj, Nicholas A. Zumwalde, Arvinder Kapur, Manish Patankar, Jenny E. Gumperz

jegumperz@wisc.edu

Highlights

Homeostatic signals drive differentiation of memory phenotype (MP) T cells

MP cells have a distinctive metabolic profile with high mitochondrial activity

They are activated by weak TCR stimulation from autologous transformed cells

Their use of glutamine suggests they act under different conditions than effectors

Bharadwaj et al., iScience 27, 109775
May 17, 2024 © 2024 The Author(s). Published by Elsevier Inc.
https://doi.org/10.1016/j.isci.2024.109775

iScience

CellPress
OPEN ACCESS

Article

Human CD4$^+$ memory phenotype T cells use mitochondrial metabolism to generate sensitive IFN-γ responses

Nikhila S. Bharadwaj,[1] Nicholas A. Zumwalde,[2] Arvinder Kapur,[3] Manish Patankar,[4] and Jenny E. Gumperz[1,5,*]

SUMMARY

The transition of naive T lymphocytes into antigenically activated effector cells is associated with a metabolic shift from oxidative phosphorylation to aerobic glycolysis. This shift facilitates production of the key anti-tumor cytokine interferon (IFN)-γ; however, an associated loss of mitochondrial efficiency in effector T cells ultimately limits anti-tumor immunity. Memory phenotype (MP) T cells are a newly recognized subset that arises through homeostatic activation signals following hematopoietic transplantation. We show here that human CD4$^+$ MP cell differentiation is associated with increased glycolytic and oxidative metabolic activity, but MP cells retain less compromised mitochondria compared to effector CD4$^+$ T cells, and their IFN-γ response is less dependent on glucose and more reliant on glutamine. MP cells also produced IFN-γ more efficiently in response to weak T cell receptor (TCR) agonism than effectors and mediated stronger responses to transformed B cells. MP cells may thus be particularly well suited to carry out sustained immunosurveillance against neoplastic cells.

INTRODUCTION

T cell production of the cytokine interferon (IFN)-γ plays a key role in both tumor control and graft-mediated pathology following hematopoietic transplantation.[1] CD4$^+$ T cells become T_{H1} cells, a major IFN-γ-producing effector population, through the integration of activation-induced metabolic and epigenetic changes during their differentiation. Naive CD4$^+$ T cells are characterized by metabolic quiescence and a "closed" chromatin structure that limits production of effector cytokines.[2,3] Upon antigen-driven activation, they upregulate their metabolic activity and undergo rapid proliferation and chromatin remodeling to become effectors.[4] Polarization into an IFN-γ-producing T_{H1} phenotype occurs in situations where high-affinity antigens, co-stimulatory signals from antigen-presenting cells, and appropriate cytokines (e.g., interleukin [IL]-12) are all concurrently present.[5] However, it has recently become clear that naive CD4$^+$ T cells can also transition to IFN-γ-producing cells in response to homeostatic signals that likely provide only weak T cell receptor (TCR) stimulation with little co-stimulation, and without the presence of IL-12.[6] CD4$^+$ T cells that follow this route have been termed "memory phenotype" (MP) cells.[7,8] MP cells play important roles in host defense against microbial infections[9,10] and may also contribute to immune-mediated pathologies.[11–14] However, little is known about what distinguishes the IFN-γ responses of MP cells from those of foreign antigen-driven T cells.

A key distinction is that MP cells differentiate in response to homeostatic signals. It is now well established that homeostatic proliferation plays a central role in the expansion of T cell populations under lymphopenic conditions.[15] Two distinct types of homeostatic proliferation have been delineated: one involving rapid T cell proliferation and one in which proliferation occurs more slowly.[16] Slow homeostatic proliferation is not associated with the acquisition of effector functions by naive T cells, whereas CD4$^+$ T cells that undergo rapid homeostatic proliferation gain the ability to produce IFN-γ and upregulate cell surface markers associated with activation. T_{H1} differentiation of these rapid proliferators is dependent on antigen-presenting cells expressing self-major histocompatibility complex (MHC) class II molecules. Presentation of self-peptides appears to be sufficient, although differentiation may be facilitated by peptides derived from commensal microbes.[17–22] Due to the abundant niche space found in lymphopenic environments, which enhances availability of homeostatic stimuli (e.g., Notch ligands, IL-7), a substantial proportion of CD4$^+$ T cells rapidly proliferate and differentiate into MP cells in these settings. Since lymphodepleting induction therapies are commonly performed prior to hematopoietic transplantation protocols,[23] MP cells likely comprise a significant portion of the T cells that arise during immune reconstitution, and IFN-γ production by these cells may thus play a key role in graft-versus-leukemia or graft-versus-host responses.

[1]Department of Medical Microbiology and Immunology, University of Wisconsin School of Medicine and Public Health; Madison, WI 53706, USA
[2]Department of Genetics, University of Wisconsin School of Medicine and Public Health; Madison, WI 53706, USA
[3]QIAGEN Sciences Inc., 19300 Germantown Road, Germantown, MD 20874, USA
[4]Department of Obstetrics and Gynecology, University of Wisconsin School of Medicine and Public Health; Madison, WI 53706, USA
[5]Lead contact
*Correspondence: jegumperz@wisc.edu
https://doi.org/10.1016/j.isci.2024.109775

This is an open access article under the CC BY-NC-ND license (http://creativecommons.org/licenses/by-nc-nd/4.0/).

The metabolic requirements for IFN-γ production by MP cells are not clear. A metabolic switch to aerobic glycolysis is considered critical for the effector functioning of antigen-driven T_{H1} cells because IFN-γ production is mechanistically linked to elevated cytoplasmic glycolytic activity.[24,25] TCR signaling has been found to contribute directly to the glycolytic switch,[26] and the strength of TCR signaling has been shown to play a key role in the fate of differentiated $CD4^+$ T cells, with strong signaling favoring a short-term T_{H1} effector state and weaker signaling tending to promote differentiation of longer-lived cell types.[27] Thus, while strong antigenic stimulation induces the acquisition of a glycolytic profile that underpins T_{H1} effector functioning, it is less clear whether the homeostatic signals encountered by MP cells promote a similar set of changes. Here, we investigated IFN-γ production by umbilical cord blood-derived human $CD4^+$ T cells that differentiate in response to signals provided by autologous antigen-presenting cells. Our results indicate that the resulting human MP cells operate under a distinctive metabolic program. Instead of relying primarily on glucose consumption as is characteristic of effector T cells that have entered a trajectory toward terminal differentiation, MP cells maintain a mitochondrially active metabolic profile and show highly sensitive TCR responsiveness. As a result, MP cells may carry out innate-like responses that do not depend on foreign antigens, and they may be particularly well situated to provide sustained surveillance that eliminates transformed cells arising over time.

RESULTS

$CD4^+$ T cells from human umbilical cord blood are recent thymic emigrants that lack the ability to produce effector cytokines

In order to avoid confounding effects from antigen-experienced T cells, we used human umbilical cord blood for these studies. In contrast to adult peripheral blood where only about 50% of the $CD4^+$ T cells have a $CD45RA^+CD45RO^-$ naive phenotype, nearly 100% of the $CD4^+$ T cells in human umbilical cord blood are $CD45RA^+CD45RO^-$ (Figure 1A). Moreover, we consistently found that over 80% of the $CD4^+$ T cells in cord blood expressed CD31, indicating they are recent thymic emigrants (RTEs),[28] whereas the frequency of $CD31^+$ cells in the naive $CD4^+$ T cell population of adult samples was variable (Figure 1A). Prior studies have established that human umbilical cord blood $CD4^+$ T cells show reduced effector cytokine production compared to naive T cells from adults.[29–31] It is not clear whether this is due to suppression (e.g., as a result of exposure to inhibitory factors or regulatory T cells) or whether this simply reflects their highly naive status. To clarify this, we compared cytokine production by cord $CD4^+$ T cells to that of adult $CD4^+$ RTEs in response to 4 h PMA and ionomycin stimulation. Intracellular cytokine staining analysis revealed little or no production of IFN-γ, IL-4, IL-13, IL-17A, or IL-10 by either cord blood $CD4^+$ T cells or adult $CD4^+$ RTEs, although adult $CD4^+$ RTEs contained slightly higher frequencies of IFN-γ-producing cells than cord blood, and cord $CD4^+$ T cells showed slightly higher frequencies of IL-17A-producing cells than adult $CD4^+$ RTEs (Figure 1B). In contrast, substantial proportions producing tumor necrosis factor alpha (TNF-α), IL-8, and IL-2 were detectable among both cord $CD4^+$ T cells and adult RTEs, with no significant differences in frequency between the two sets of samples (Figure 1B). Thus, the cytokine profile of $CD4^+$ T cells from umbilical cord blood appeared similar to that of adult RTEs in that they both generally lacked the ability to rapidly produce effector cytokines, but they readily produced IL-2 and the inflammatory cytokines TNF-α and IL-8. Analysis of T_{reg} frequencies ($CD4^+$ T cells with a $CD25^+CD127^{lo}$ surface phenotype and elevated intracellular expression of FoxP3) did not reveal a significant difference between cord blood samples and adult peripheral blood mononuclear cells (PBMCs) (Figure 1C). Together, these results indicate that human umbilical cord blood is highly enriched for naive T cells that have not yet acquired the capacity to rapidly produce effector cytokines.

Transplanted naive human $CD4^+$ T cells acquire T_{H1} characteristics in a pathogen-independent manner

We next sought to assess transition into an IFN-γ-producing phenotype following transplantation into a lymphopenic environment. To do this, we transplanted human cord blood mononuclear cells (CBMCs) into non-conditioned non-obese diabetic (NOD)/severe combined immunodeficiency (SCID)/$\gamma_c^{-/-}$ (NSG) mice. We have previously established that by minimizing the damage-associated inflammation resulting from conditioning there is little or no graft-versus-host-disease (GVHD) for at least 6 weeks following transplantation of CBMCs, and thus this system mainly models human T cell activation due to introduction into a lymphopenic environment.[32,33] To investigate the impact of pathogen exposure, in parallel we similarly transplanted CBMCs that were briefly exposed to Epstein-Barr virus (EBV), a human-specific virus that infects B cells within the CBMC sample and drives their neoplastic transformation *in vivo* following transplantation.[34] Splenocytes were harvested after one, three, or five weeks, and human $CD4^+$ T cells were analyzed flow cytometrically to assess their capacity for cytokine expression after short-term (4 h) PMA/ionomycin treatment. We found that the frequency of $CD4^+$ T cells capable of rapidly producing IFN-γ increased over the first 3 weeks following transplantation and that it appeared similar for mice transplanted with EBV-infected versus uninfected CBMCs (Figure 2A). T cells showing an ability to rapidly produce TNF-α did not markedly increase (Figure 2A), and there was little or no detectable production of type 2 cytokines such as IL-13 in either condition (Figure S1). Thus, T cells transplanted in both the uninfected and virally infected conditions selectively acquired an IFN-γ-producing phenotype. By 4 weeks post-transplantation $CD4^+$ T cells in both the uninfected and EBV-infected conditions also showed detectable expression of the transcription factor T-bet (Figure 2B) and of the IL-12 receptor beta 2 chain (IL-12Rβ2) (Figure 2C), both of which play critical roles in T_{H1} differentiation.[35,36] Since $CD4^+$ T cells in the uninfected condition showed comparable changes to those in the EBV-infected condition (Figures 2B and 2C), these results indicated that T_{H1} differentiation following transplantation occurred even in the absence of infection.

To further investigate the T cell differentiation that occurred in the absence of pathogenic challenge, we assessed the status of the T cells over time following transplantation of uninfected CBMCs into NSG mice. This analysis revealed that both $CD4^+$ and $CD8^+$ T cells underwent a linear rate of doubling over the first 4 weeks (Figure 2D). During this time, nearly all of the $CD4^+$ T cells transitioned to an experienced cell surface phenotype characterized by loss of both CD45RA and CD62L (Figures 2D and 2E). Together, these findings indicated that damage-associated inflammation and pathogen exposure were not required for human cord blood $CD4^+$ T cells to acquire a T_{H1} phenotype following

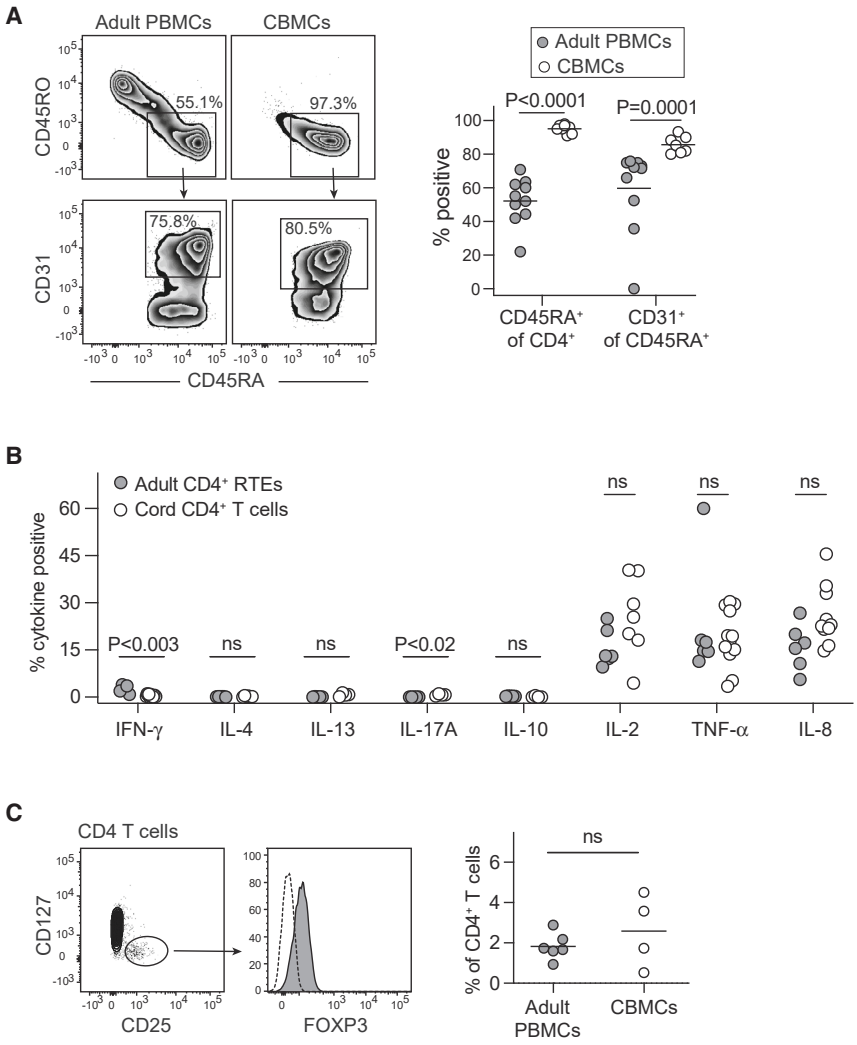

Figure 1. CD4$^+$ T cells from cord blood are enriched for recent thymic emigrants and do not produce effector cytokines

(A) Representative flow cytometric staining of CD4$^+$ T cells isolated from human umbilical cord blood or adult peripheral blood. CD45RA and CD45RO were used to identify naive cells (top row); CD31 expression within the naive population was assessed to identify recent thymic emigrants (RTEs). Scatterplot on right shows aggregated results from 10 PBMC and 8 cord blood samples. *p* values determined using Mann-Whitney analysis.

(B) Analysis of intracellular cytokine expression by CD4$^+$ T cells from cord blood, or CD4$^+$ RTE population from adult blood, after 4 h PMA/ionomycin stimulation. *p* values determined using Mann-Whitney analysis.

(C) Representative flow cytometric analysis used to identify T_{regs} (CD25$^+$CD127^{lo}) and FoxP3 staining (filled histogram) compared to isotype (dotted line) of the gated population. Scatterplot on right shows percent T_{regs} within the CD4$^+$ T cell population of cord or adult blood samples.

transplantation into a lymphopenic environment. However, an important caveat of this analysis is clearly that the role of xenoantigenic stimulation in this model remains unclear.

Exposure to autologous antigen presenting cells induces transition to MP

We therefore next used an *in vitro* model where we could more rigorously control the nature of the stimulation received by the naive human T cells. CD4$^+$ T cells were purified from cord blood, labeled with cell trace violet (CTV), and cultured in parallel in three different conditions as follows: *i*) with homeostatic cytokines (IL-7 and IL-2) alone; *ii)* with homeostatic cytokines and autologous monocytes (to provide self-MHC class II and adhesion ligands); and *iii*) with homeostatic cytokines, anti-CD3 and anti-CD28 antibodies, and plate-bound recombinant ICAM-1-Fc fusion protein (to provide strong TCR stimulation, co-stimulation, and an adhesion ligand). The T cells were exposed to these culture conditions for 3–5 days, then transferred to new wells containing only IL-2/IL-7 medium, and "rested" until day 10. Flow cytometric analysis revealed that a fraction of the T cells that were cultured the whole time only with IL-7 and IL-2 had undergone a few rounds of proliferation, but they maintained a naive phenotype of high CD45RA and low CD45RO and showed little or no downregulation of CD31 (Figure 3A). As

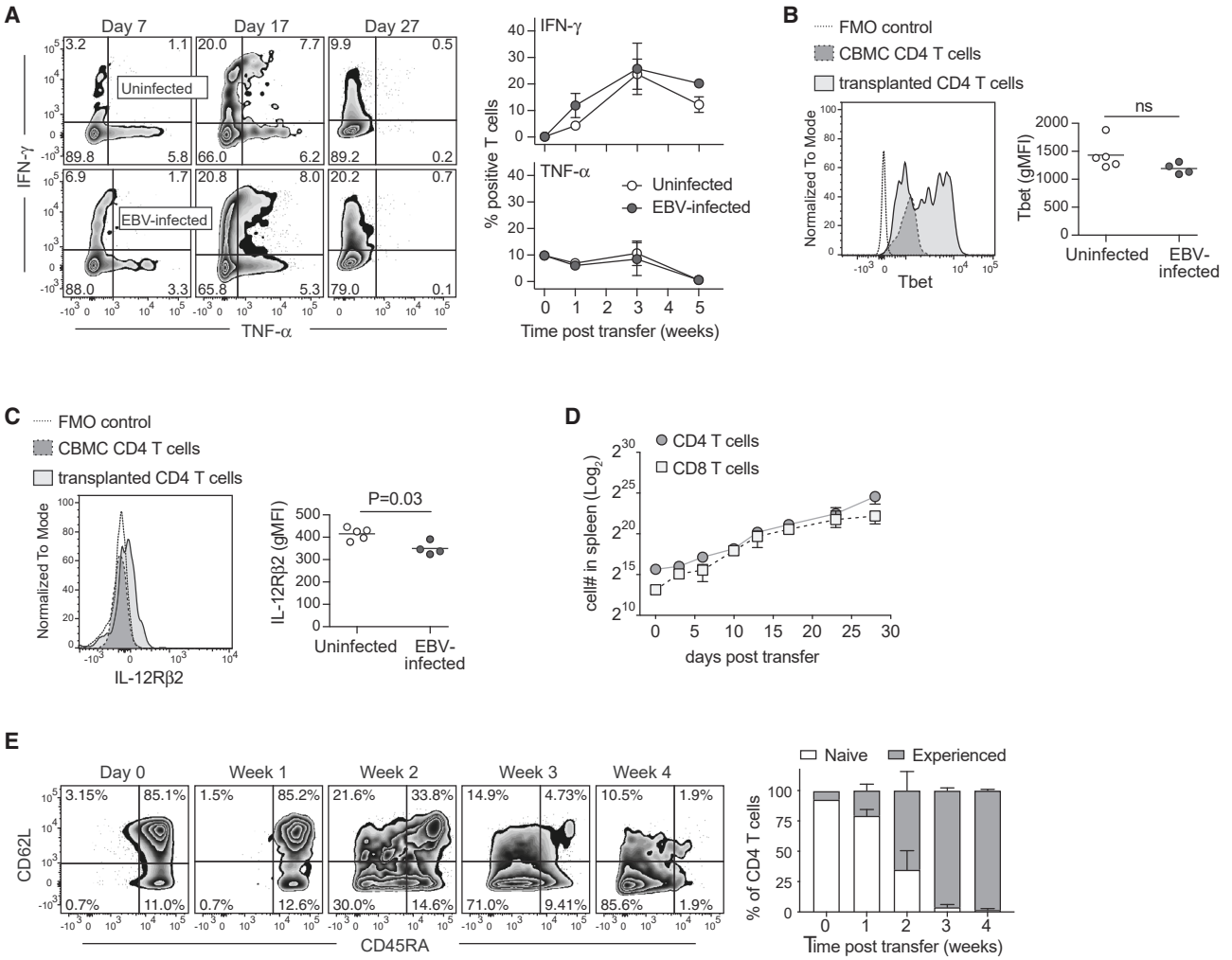

Figure 2. Transplanted naive human CD4$^+$ T cells acquire effector characteristics in a pathogen-independent manner

EBV-infected or mock-treated CBMCs were administered to NSG mice.

(A) Murine splenocytes were harvested at indicated times after transplantation and stimulated with PMA/ionomycin for 4 h. Representative flow cytometric staining is shown for intracellular IFN-γ and TNF-α within the CD4$^+$ T cell population. Plots on right show means ± SD for 2–3 mice.

(B) Representative flow cytometric staining for intracellular expression of T-bet. Filled histograms show CD4 T cells in starting CBMC sample (dark gray) and in CD4 T cells from transplanted mice (light gray); open histogram with dotted line shows fluorescence minus one (FMO) control staining for CD4 T cells from transplanted mice. Plot on right shows aggregated results for samples from uninfected and EBV-infected mice collected at 4 weeks post-injection.

(C) Representative flow cytometric analysis and aggregated results for cell surface IL-12Rβ2. *p* value detemined using Mann-Whitney analysis.

(D) Quantitation of the total numbers of human CD4$^+$ and CD8$^+$ T cells in the murine spleen following transplantation of uninfected CBMCs. Symbols represent means ± SD of 2–6 mice.

(E) Representative flow cytometric staining showing CD45RA and CD62L expression by human CD4$^+$ T cells in murine spleen at the indicated times post-transplant. Plot on right shows proportions of naive (CD45RA$^+$) and experienced (CD45RA$^-$) human CD4$^+$ T cells at each time point; bars represent means ± SD from 3 mice.

See also Figure S1.

expected, the T cells exposed to anti-CD3/CD28 and plate-bound ICAM-1-Fc underwent many rounds of proliferation and acquired an experienced phenotype as indicated by loss of CD45RA, acquisition of CD45RO, and downregulation of CD31 (Figure 3A). Co-culture with autologous monocytes induced many rounds of proliferation by a fraction of the T cells, and a significant fraction of the cells lost expression of CD45RA and CD31 and gained CD45RO (Figure 3A).

Next, we assessed the ability of the CD4$^+$ T cells in these culture conditions to rapidly produce IFN-γ in response to short-term (4 h) PMA and ionomycin stimulation. T cells that were cultured with homeostatic cytokines alone resembled freshly isolated cord blood T cells in that they produced little or no detectable IFN-γ (Figure 3B). In contrast, a substantial fraction of the T cells cultured with anti-CD3/CD28 and ICAM-Fc were able to produce IFN-γ in this assay (Figure 3B). A significant proportion of the T cells that were exposed to autologous monocytes had

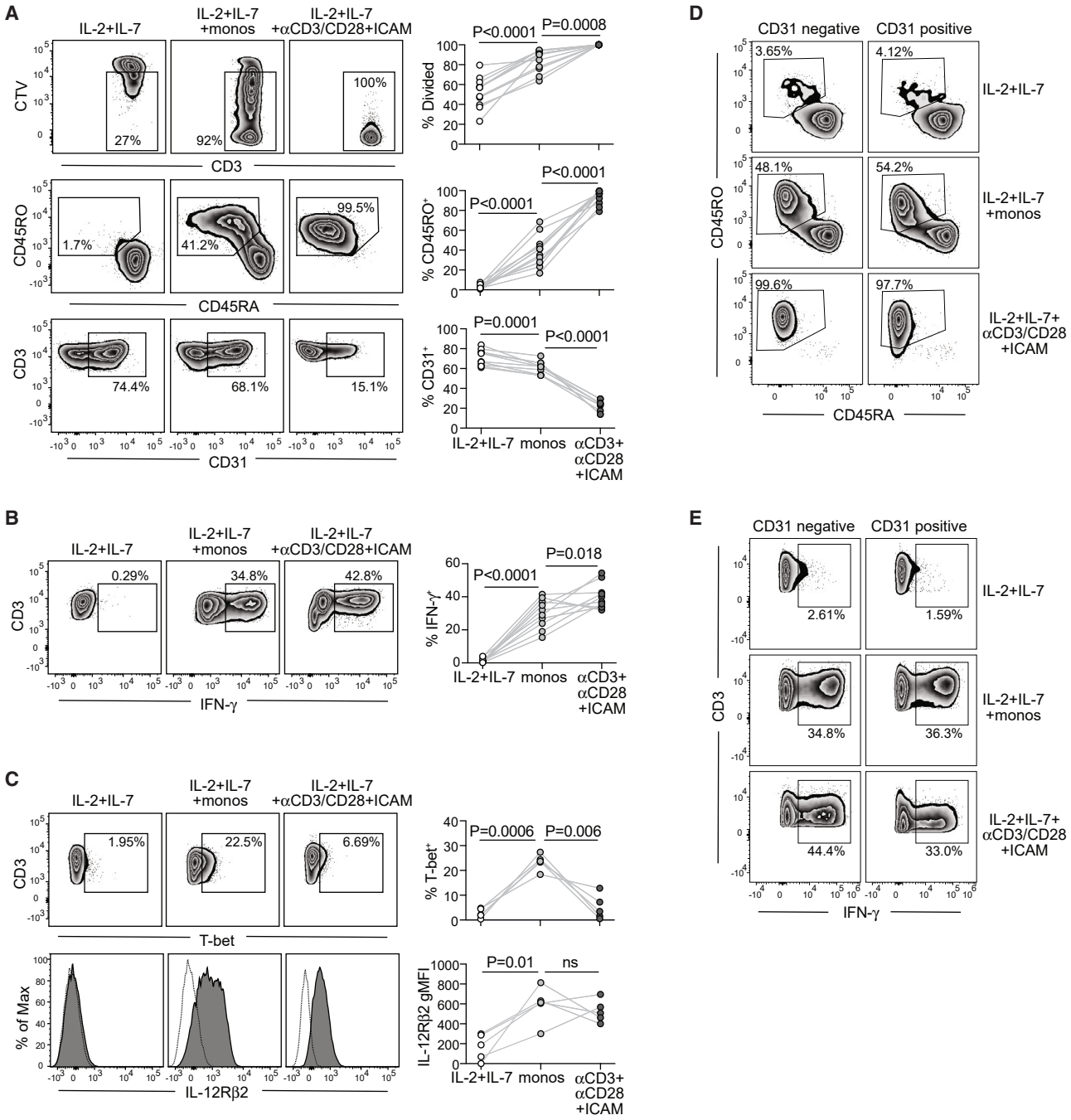

Figure 3. A fraction of CD4⁺ cord T cells differentiate into MP cells through exposure to homeostatic signals

Cord blood CD4⁺ T cells were cultured for 3–5 days in medium containing IL-2 and IL-7 alone, or with autologous monocytes, or with anti-CD3, anti-CD28, and plate-bound ICAM-1 Fc, then removed to new wells and rested in IL-2/IL-7 medium until day 10.

(A) Top row: T cell proliferation assessed by dilution of cell trace violet (CTV); middle row: experience assessed by CD45RA and CD45RO; bottom row: RTE status assessed by CD31.

(A-C) plots on right show aggregated results from independent analyses of independent cord blood samples, with *p* values determined using two-tailed paired t-tests.

(B) Intracellular IFN-γ expression after 4 h PMA/ionomycin stimulation.

(C) Top row: staining for intracellular expression of T-bet; bottom row: staining for cell surface IL-12Rβ2 (filled histograms) and isotype control (dotted lines).

(D) and (E) CD4⁺ cord blood T cells were magnetically sorted to isolate CD31⁺ and CD31⁻subsets, then subjected to the culture conditions described above. Flow cytometric analysis was performed to determine the percent of cells that transitioned to an experienced (CD45RO⁺CD45RA⁻) phenotype (D), or that produced IFN-γ after 4 h PMA/ionomycin stimulation (E).

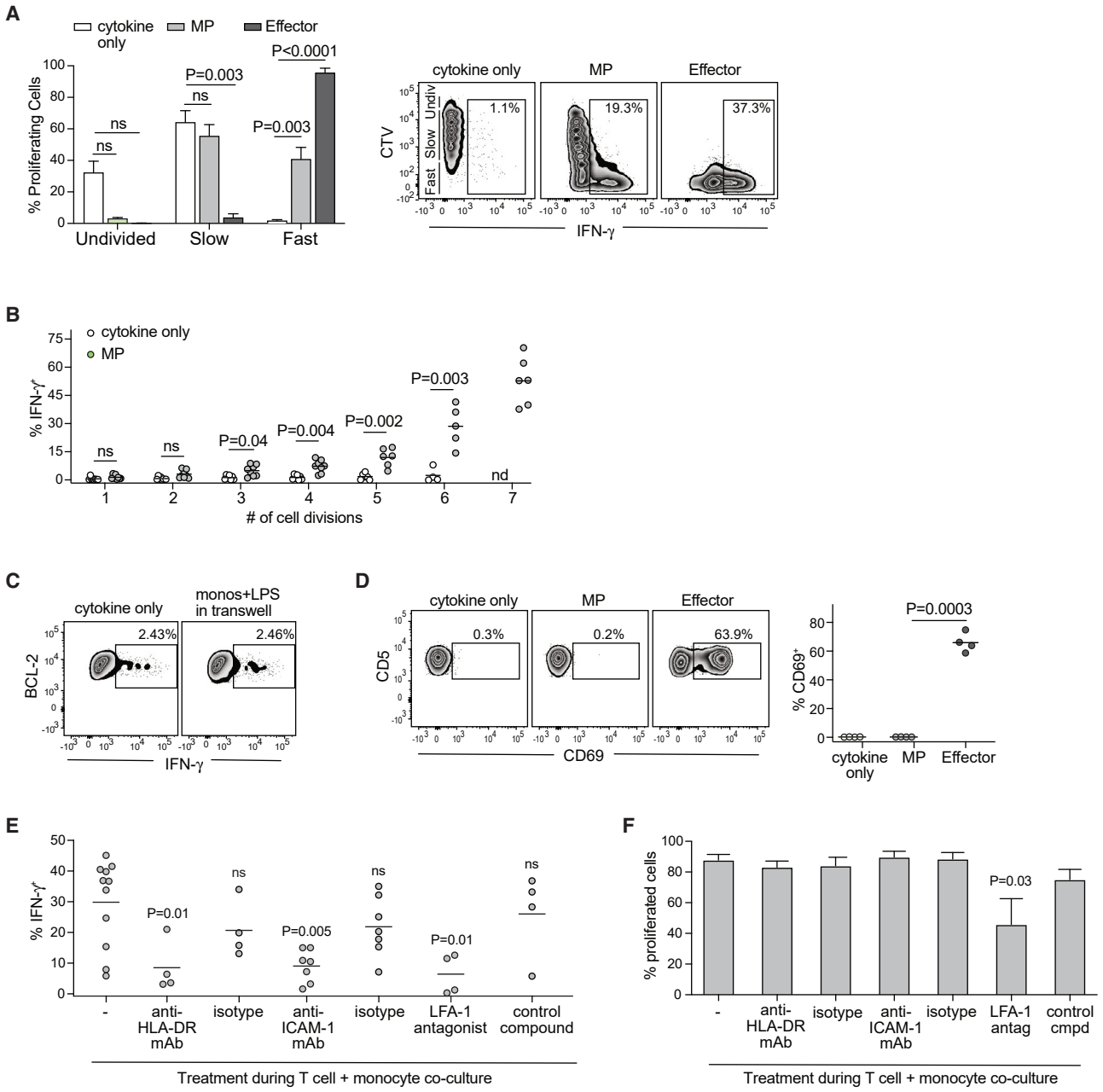

Figure 4. MP cell acquisition of capacity to produce IFN-γ is associated with rapid homeostatic proliferation and dependent on access to self-MHC

Cord blood CD4$^+$ T cells were labeled with CTV and cultured for 5–7 days in medium containing IL-2 and IL-7 alone (cytokine only), or with autologous monocytes (MP), or with anti-CD3/CD28 and ICAM-1-Fc (Effector), and the number of rounds of division and intracellular IFN-γ expression following 4 h PMA/ionomycin stimulation were assessed by flow cytometry.

(A) Bar plot shows percent of cells that underwent >6 rounds of division (Fast); or ≤6 rounds of division (Slow); or that remained undivided. Results represent means ± SEM from 5 to 10 independent analyses, *p* values determined using two-tailed paired t-tests. Panels on right show representative flow cytometric staining results.

(B) Percent IFN-γ$^+$ MP cells (dark symbols) or T cells cultured in cytokine only (light symbols) detected at each of the indicated number of cell divisions, *p* values determined using two-tailed paired t-tests.

(C) Cord blood CD4$^+$ T cells were cultured in medium containing IL-2 and IL-7 in the presence or absence of a transwell insert containing LPS-stimulated monocytes for the first 5 days, and intracellular expression of IFN-γ was determined on day 7 after 4 h PMA/ionomycin stimulation.

(D) Cell surface expression of CD69 after 24 h of culture in the indicated conditions. Plot on right shows aggregated results from 4 independent cord blood samples, with *p* value determined using two-tailed upaired t-test.

Figure 4. *Continued*

(E) and (F) T cells were cultured for 3 days with autologous monocytes alone or in the presence of blocking antibodies against MHC class II or ICAM-1 or isotype-matched negative controls, or in the presence of the LFA-1 small molecule antagonist (BI-1950) or the negative control compound (BI-9446), and then were rested in cytokine medium alone for an additional 4 days (E) Percent of T cells expressing intracellular IFN-γ after 4 h PMA/ionomycin stimulation. *p* values determined using two-tailed unpaired t-tests. (F) Percent of T cells showing reduced levels of CTV. Bars represent means ± SEM from 4 to 7 independent analyses. *p* value determined using two-tailed unpaired t-test.

also acquired the ability to rapidly produce IFN-γ (Figure 3B). Additionally, the monocyte-exposed T cells showed upregulation of cell surface IL-12 receptor (IL-12Rβ2) and intracellular expression of T-bet, indicating T_{H1}-polarization (Figure 3C).

Thus, a fraction of the T cells that were exposed to autologous monocytes acquired an experienced T_{H1} phenotype that included the ability to rapidly produce IFN-γ. We considered this fraction of the monocyte-exposed T cells to represent MP cells, whereas the T cells that were activated by anti-CD3/CD28 and ICAM-Fc were more similar to conventional T_{H1} effector cells, and $CD4^+$ cord T cells cultured in homeostatic cytokines alone remained unpolarized. To investigate whether MP cells arose from the more mature naive fraction within the starting cord blood T cell population (i.e., the approximately 20% that had lost CD31 but expressed CD45RA and lacked CD45RO, as seen in Figure 1A) or whether RTEs could also give rise to MP cells, we purified CD31-positive and -negative $CD45RA^+$ subsets from CBMCs by magnetic sorting and subjected them to the three differentiation conditions. The CD31-positive and -negative starting populations showed nearly identical changes in cell surface phenotype and acquisition of capacity to produce IFN-γ (Figures 3D and 3E), indicating that both RTEs and mature naive T cells were similarly capable of differentiating into MP cells.

MP cell polarization is dependent on self-MHC-driven fast homeostatic proliferation

It has been previously established that the capacity to produce IFN-γ increases as a function of cell division during T_{H1} differentiation.[37,38] We therefore investigated this relationship for the three types of T cells generated in our culture conditions. We evaluated the rate of proliferation by analyzing the amount of CTV dilution over time, focusing on early time points (e.g., day 3–7) in order to visualize the fraction of cells that were proliferating rapidly. Fast proliferation was defined as having undergone one or more rounds of division every 24 h, while slow proliferators underwent at least 1 and less than 7 rounds of division in 7 days, and T cells that showed no evidence of any CTV dilution at all were classified as undivided. T cells cultured with IL-2 and IL-7 alone almost entirely lacked fast proliferators, and, while many of the cells showed evidence of slow proliferation, these cultures often retained some undivided cells (Figure 4A). Monocyte-exposed T cells showed a mixture of slow and fast proliferating T cells with little or no evidence of undivided cells, while stimulation by anti-CD3/anti-CD28 and ICAM-Fc led to almost exclusively fast proliferating T cells (Figure 4A). Interestingly, T cells cultured with cytokines only and those in the MP cultures differed in the relationship between cell division and IFN-γ production. In the MP cultures, T cells that underwent at least 3 rounds of cell division showed significantly increased IFN-γ production, whereas, in the cytokine-only condition even when T cells underwent as many as 6 rounds of cell division, they still showed little or no evidence of IFN-γ production (Figure 4B). MP cells that underwent at least 7 rounds of cell division showed a similar capacity to produce IFN-γ as those in the effector T cell condition (compare Figures 3B and 4B). We also noted that upregulation of T-bet and IL-12RB in the MP cultures appeared largely limited to the T cells that had undergone fast homeostatic proliferation (data not shown). Together these results suggested that differentiation into a T_{H1}-like status was associated not just with the total number of rounds of cell division but also with undergoing fast rather than slow homeostatic proliferation.

We next assessed the nature of the stimulation required for MP cell production of IFN-γ. Acquisition of the ability to produce IFN-γ appeared to require cell contact with monocytes, since exposure to soluble factors produced by activated monocytes in a transwell insert did not result in an increased frequency of IFN-γ-producing T cells (Figure 4C). We also noted that, in contrast to effector cells, which showed clearly upregulated levels of cell surface CD69 after 24 h, MP cells resembled T cells cultured with cytokines only in that both lacked cell surface expression of CD69 (Figure 4D). Since CD69 is upregulated by TCR stimulation in a dose-dependent manner,[39] their lack of CD69 expression suggested that the MP cells had not received a strong TCR signal. We therefore investigated whether binding to MHC class II molecules during their differentiation in co-cultures with autologous monocytes was required for T cell acquisition of the capacity to produce IFN-γ. Inclusion of anti-MHC class II blocking antibodies (pan-specific for HLA-DR) in the co-cultures resulted in significantly reduced frequencies of IFN-γ-producing cells compared to control T cells co-cultured with monocytes in the absence of a blocking monoclonal antibody (mAb), whereas the presence of an isotype control mAb did not result in reduced IFN-γ production (Figure 4E). We also found that preventing T cell adhesion to monocytes by disrupting LFA-1 integrin-mediated binding resulted in significantly reduced ability to produce IFN-γ, since the presence of a blocking antibody against ICAM-1 or the presence of a small molecule antagonist of LFA-1 (BI-1950) also resulted in significantly reduced frequencies of IFN-γ-producing cells (Figure 4E). Inclusion of blocking antibodies against MHCII or ICAM-1 did not affect the amount of T cell proliferation, while addition of the BI-1950 small molecule LFA-1 antagonist but not the negative control compound resulted in ~50% reduced proliferation (Figure 4F). These results indicated that signals derived from access to self-MHC class II molecules were important for MP cells that underwent fast homeostatic proliferation to become polarized to a T_{H1}-like phenotype that can rapidly produce IFN-γ.

MP cells show elevated responsiveness to weak TCR stimulation

To assess their functional activity, we investigated the ability of T cells from the three culture conditions to produce IFN-γ in response to B lymphoblastoid tumor spheroids. Infection of cord blood B lymphocytes with EBV results in their neoplastic transformation into

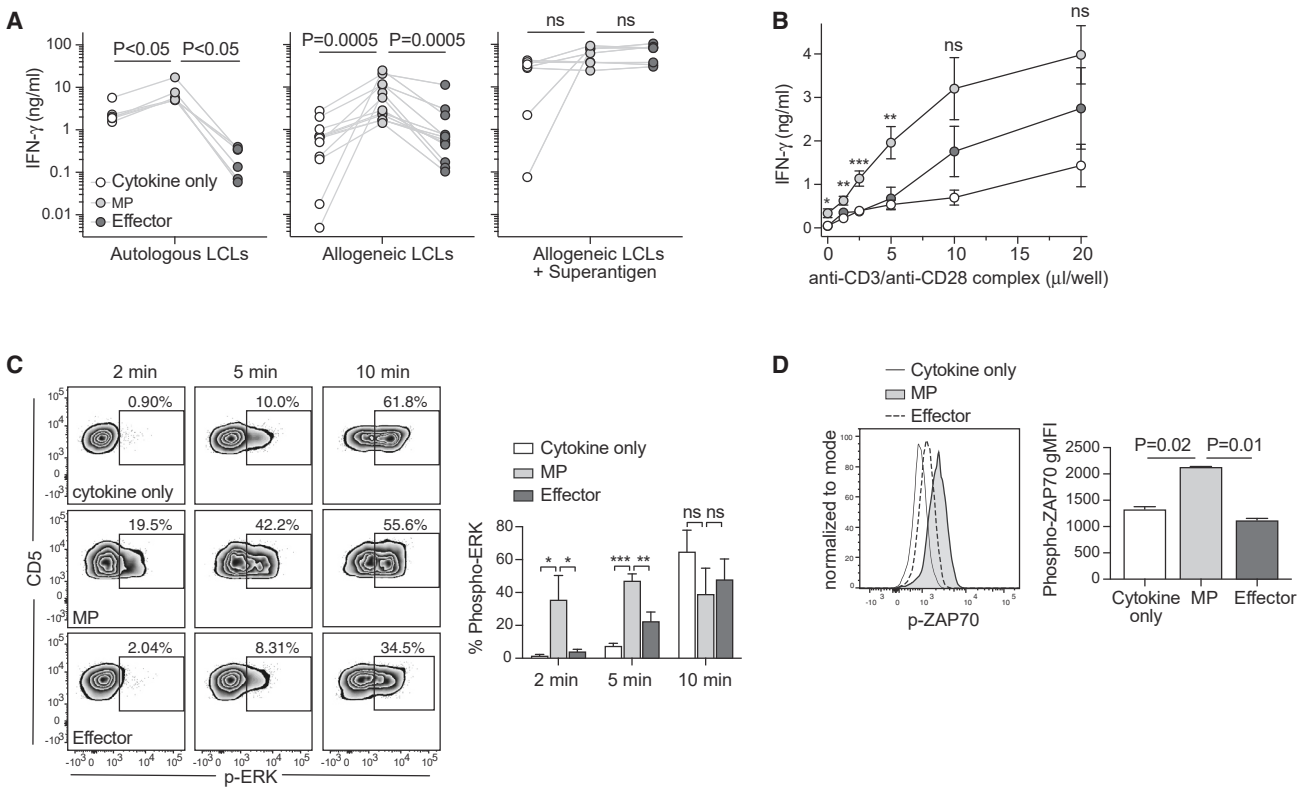

Figure 5. MP cells show elevated TCR responsiveness

(A) T cells were co-incubated with autologous LCLs (left plot), or allogeneic LCLs (middle plot), or allogeneic LCLs treated with superantigen (right plot), and IFN-γ in the culture supernatant was quantitated after 24–48 h. *p* values determined using two-tailed paired t-tests.

(B) T cells were stimulated with the indicated doses of anti-CD3/anti-CD28 antibody complex and secreted IFN-γ was quantitated after 24 h. Plot shows means ± SEM of 8 independent experiments; asterisks indicate statistical significance (* = $p \leq 0.05$; ** = $p \leq 0.01$; *** = $p \leq 0.001$) for paired t test comparisons of MP cells with effector T cells.

(C) The indicated T cell cultures were stimulated with 5 µL anti-CD3/anti-CD28 antibody complex for the lengths of time indicated, and ERK phosphorylation was assessed by flow cytometry. Bar plot shows means ± SD of 3 replicates, with *p* values determined by two-tailed unpaired t-tests.

(D) Representative results for intracellular phospho-ZAP-70 staining after 2 min stimulation with 5 µL anti-CD3/anti-CD28 antibody complex. Bar plot shows means ± SD of 2 replicates, with *p* values determined by two-tailed unpaired t-tests.

See also Figures S2 and S3.

lymphoblastoid cell lines (LCLs) that self-adhere into small tumor spheroids (Figure S2). The T cells were co-cultured with autologous, or allogeneic, or superantigen-treated allogeneic LCLs, and culture supernatants were tested for IFN-γ by ELISA after 24–48 h. Remarkably, MP cells produced significantly greater amounts of IFN-γ in response to autologous or allogeneic LCLs compared to either the naive or the effector T cells (Figure 5A). However, when co-cultured with superantigen-treated LCLs, T cells from all three differentiation conditions responded strongly (Figure 5A). These results indicated that T cells from all three conditions were capable of secreting IFN-γ within 24–48 h when challenged with a strong TCR agonist (superantigen) but suggested that MP cells have an enhanced ability to respond to the weaker TCR stimulation provided by autologous or allogeneic LCLs.

To directly investigate the impact of the strength of TCR stimulation, rested T cells from each of the three differentiation conditions were exposed to titrated doses of anti-CD3/anti-CD28 multimer for 24 h; then supernatants were tested for IFN-γ by ELISA. This analysis confirmed that the MP cells produced significantly greater amounts of IFN-γ in response to suboptimal levels of TCR stimulation (Figure 5B). We also found that this was the case regardless of whether the MP cells were generated from the $CD31^{+}$ or $CD31^{-}$ subset of cord T cells (Figure S3). We next assessed the kinetics of ERK phosphorylation in response to CD3/CD28 stimulation. Rested T cells from the three differentiation conditions were exposed to a suboptimal (5 µL) dose of anti-CD3/anti-CD28 multimer for short times (2–10 min) and then immediately placed on ice and fixed and permeabilized for flow cytometric analysis of phospho-ERK levels. This revealed that ERK phosphorylation occurred more quickly in MP cells compared to either naive or effector cells (Figure 5C). A similar analysis of ZAP-70 phosphorylation demonstrated that MP cells showed a higher level of phospho-Zap-70 after 2 min of suboptimal CD3/CD28 stimulation than either naive or effector cells (Figure 5D). These results indicated that TCR signaling activation occurs more rapidly in MP cells following a suboptimal stimulus, which may account for their increased IFN-γ production in response to weak TCR agonism.

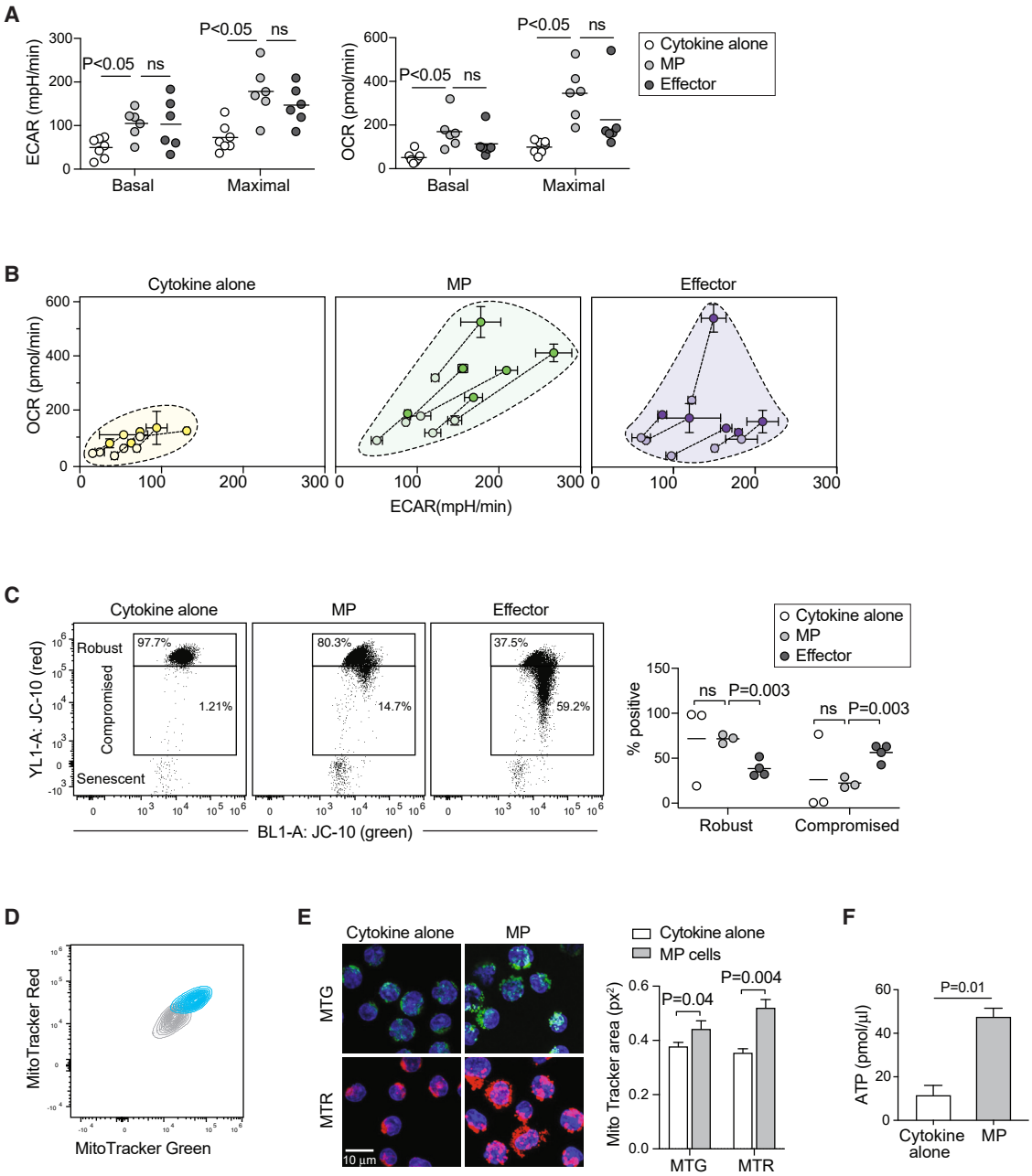

Figure 6. MP differentiation is associated with changes to metabolic phenotype and mitochondrial status

(A) Rates of glycolysis and oxidative metabolism were assessed by analysis of extracellular flux under basal conditions and under maximal stress induced by addition of oligomycin and FCCP. Left plot shows extracellular acidification rates (ECAR) and right plot shows oxygen consumption rates (OCR) from 6 independent experiments. *p* values determined by two-tailed paired t-tests.

(B) Summary plots showing ECAR on the x axis and OCR on the y axis for the indicated T cell cultures from 6 different cord samples. Light symbols show basal, and dark symbols show maximal rates.

(C) The JC-10 dye was used to evaluate mitochondrial membrane potential as an indicator of mitochondrial health. Left plots show representative flow cytometric results for live cells from each T cell condition, with gates drawn to identify cells containing mitochondria with high membrane potential (Robust) or where membrane potential has been lost (Compromised). Plot on right shows percent of live cells in these gates for T cells from 3 independent cord samples, with *p* values determined by two-tailed unpaired t-tests.

(D) Flow cytometric analysis of cells stained with MitoTracker Red (MTR) and Green (MTG), indicating mitochondrial activity and mass respectively, for T cells cultured in cytokine alone (gray) compared to MP cells (blue).

Figure 6. *Continued*

(E) Fluorescence microscopic images at 63X magnification, showing T cells stained with MitoTracker Green (top row) or Red (bottom row with nuclear staining by DAPI shown in blue. Bottom left image shows scale bar of 10 μm. Bar plot on right shows area of red or green staining normalized by the nuclear staining. Plot shows means +SEM of 2–5 independent experiments, with *p* values determined by two-tailed unpaired t-tests.

(F) Quantitation of ATP in T cells after 5 days of culture; results represent means ± SD of 3 replicates, *p* value determined by two-tailed unpaired t-test.

MP cells upregulate metabolic activity following differentiation

We next investigated the metabolic status of T cells from the three culture conditions. MP cells showed significantly increased basal and maximal levels of extracellular acidification rate (ECAR) and of oxygen consumption rate (OCR) compared to T cells cultured in cytokines alone, whereas MP cells and effector T cells did not differ significantly in their levels of ECAR or OCR (Figure 6A). Since OCR is proportional to mitochondrial respiration and ECAR is proportional to glycolysis, these results indicated that differentiation into the MP phenotype was accompanied by elevation of both oxidative phosphorylation (OXPHOS) and glycolysis compared to T cells that had only undergone slow homeostatic proliferation. Notably, since we performed these analyses after the MP cells had rested for at least 5 days following their exposure to autologous monocytes, these results suggest that the MP cells had undergone a durable change in metabolic state. The rested MP cells consistently showed concordant upregulation of both OCR and ECAR, whereas at this time point effector cells typically showed upregulation of ECAR with less increase in OCR. As a result, the overall metabolic profile of MP cells and effector cells appeared distinct (Figure 6B).

To further investigate, we assessed mitochondrial membrane potential using the JC-10 dye, which undergoes fluorescence changes based on the status of mitochondrial membranes. In cells with healthy mitochondria that have high membrane potential, the JC-10 dye will accumulate in the mitochondrial matrix and emit both red and green fluorescence, whereas when mitochondrial membrane potential is lost the dye will leak into the cytoplasm and lose its red fluorescence signal. While the viability appeared similar for MP and effector T cell cultures, we found that MP cultures contained a higher percentage of T cells with robust mitochondria and a lower percentage with compromised mitochondria compared to effector T cell cultures (Figure 6C). T cells cultured in cytokine alone were variable in regards to mitochondrial status by this assay (Figure 6C). To further assess mitochondrial differences between MP cells and T cells cultured in cytokine alone, we co-labeled the cells with MitoTracker Green (which stains all mitochondria) and MitoTracker Red (which stains in proportion to mitochondrial membrane potential). Flow cytometric analysis showed a clear shift in both channels, suggesting not only that MP cells had more mitochondrial biomass per cell than those cultured in cytokine alone but also that their mitochondria were also more active (Figure 6D). Microscopic imaging showed that the mitochondria of MP cells had acquired a more distinct, punctate appearance, and quantitation of the fluorescence signal confirmed that they had slightly increased total mitochondrial area, and markedly increased active mitochondrial area (Figure 6E). Consistent with greater mitochondrial activity, we also found that MP cells had higher levels of intracellular ATP than T cells cultured in cytokine alone (Figure 6F). These results demonstrate that MP cell differentiation is associated with increased mitochondrial activation, while retaining a comparatively robust mitochondrial membrane potential status.

MP cells use glutamine metabolism to fuel IFN-γ responses

We hypothesized that the elevated mitochondrial activity of MP cells may enable them to maintain IFN-γ production under hypoglycemic conditions by facilitating their use of alternative metabolic substrates. To test this, we assessed IFN-γ production by MP cells versus effector T cells under hypoglycemic conditions. MP cells and effector T cells were co-cultured for 24 h with superantigen-treated allogeneic LCLs in medium containing high (2 mM) glutamine with either high (10 mM) or low (3.5 mM) glucose; then culture supernatants were collected and secreted IFN-γ was quantitated by ELISA. As expected, IFN-γ production by the effector T cells was greatly impacted by reduced glucose availability, showing on average more than an 85% reduction (mean 11.2% ± 11.1% of high glucose amount) (Figure 7A). In contrast, MP cells typically maintained most of their IFN-γ production in low-glucose medium (65.3% ± 28.6% of high glucose amount) (Figure 7A). Since the MP cells were only partially impacted by reduced glucose availability, and it has been previously established that glutamine is a critical metabolite for T cells that have undergone ERK-mediated signaling during activation,[40] we evaluated the impact of glutamine availability on IFN-γ production. To test this, MP or effector T cells were placed into medium containing high glucose (10 mM) with normal (2 mM), reduced (1 mM), or no glutamine and stimulated with a sub-optimal anti-CD3/CD28 dose (5 μL) for 24 h. Whereas IFN-γ production by effector T cells was not diminished in medium containing reduced or no glutamine, MP cell responses were nearly 50% less in these conditions (Figure 7B).

Since glutamine is metabolized within mitochondria, we compared the impact of drugs that block glycolysis or mitochondrial metabolic processes. Using culture medium containing 10 mM glucose and 2 mM glutamine, MP cells or effector T cells were stimulated with a sub-optimal dose of anti-CD3/CD28 antibody complex in the presence or absence of a series of inhibitors as follows: *i)* 2-Deoxy-D-glucose (2-DG), a glucose analog that acts as a competitive inhibitor of glucose-6-phosphate and consequently abrogates all glycolysis; *ii*) galloflavin, a lactate dehydrogenase (LDH) inhibitor that specifically blocks glucose breakdown in the cytoplasm but does not prevent mitochondrial glucose metabolism; *iii*) UK5099, an inhibitor of the mitochondrial pyruvate carrier (MPC) that prevents mitochondrial breakdown of pyruvate and thus inhibits oxidative glycolysis; *iv*) BPTES, a selective inhibitor of the glutaminase 1 (GLS1) enzyme that is required for glutaminolysis; *v*) etomoxir (ETO), an inhibitor of CPT1A, which is a rate-limiting enzyme of fatty acid oxidation; and *vi*) oligomycin, an inhibitor of ATP synthase that therefore blocks OXPHOS. Analysis of the amounts of IFN-γ produced in the presence of these drugs compared to vehicle treatment revealed that while the effector T cells were highly sensitive to 2DG and galloflavin but nearly completely resistant to UK5099 and BPTES, IFN-γ production by the MP cells was partially inhibited by all of these compounds (Figure 7C). Neither MP nor effector T cells showed

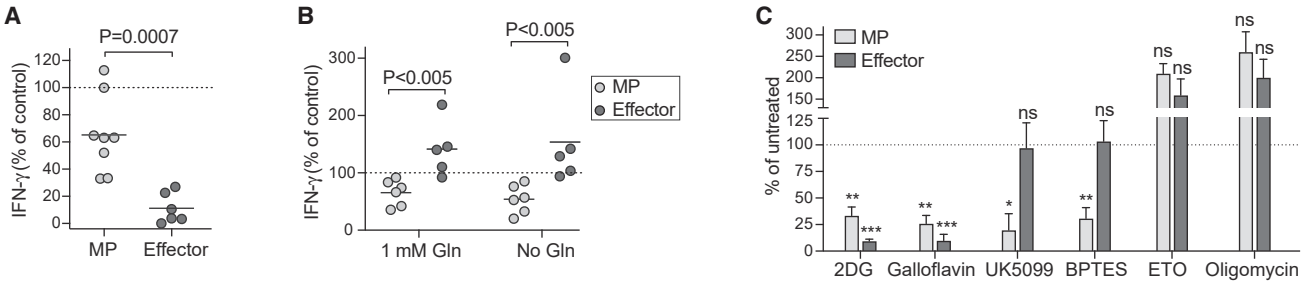

Figure 7. MP cells utilize glutamine metabolism to support IFN-γ production

(A) Analysis of ability to produce IFN-γ under conditions of limited glucose availability. Rested MP and effector T cells were co-cultured with allogeneic LCLs treated with superantigen in medium containing 2 mM glutamine and either high (10 mM) or low (3.5 mM) glucose, and secreted IFN-γ was quantified after 24 h. Plot shows IFN-γ produced under low-glucose conditions as a percentage of that produced by the same cells under high glucose conditions. Each symbol represents the results from an independent experiment. *p* value determined by two-tailed unpaired t-test.

(B) Impact of glutamine availability on IFN-γ production. T cells were stimulated with a sub-optimal dose of anti-CD3/anti-CD28 antibody complex (5 μL) in medium containing high (10 mM) glucose and either normal (2 mM), low (1 mM), or no glutamine. Plot shows amounts of IFN-γ made in reduced glutamine conditions as a percentage of amounts made in medium containing normal (2 mM) glutamine. *p* value determined by two-tailed unpaired t-test.

(C) Effects of blocking specific metabolic pathways. MP and effector T cells were stimulated with a sub-optimal dose of anti-CD3/anti-CD28 antibody complex (5 μL) in medium containing 10 mM glucose and 2 mM glutamine, in the presence of specific inhibitors (2-DG, Galloflavin, UK5099, BPTES, ETO or Oligomycin) or vehicle. Plot shows IFN-γ production in the presence of the indicated inhibitor as a percentage of the amount produced in the absence of inhibition. Results represent means ± SEM from 2 to 4 independent experiments; asterisks show significance (* = $p \leq 0.05$; ** = $p \leq 0.01$; *** = $p \leq 0.001$) based on a two-tailed one sample t test comparing each condition to 100%.

diminished IFN-γ production in the presence of ETO or oligomycin (Figure 7C). Together, these results establish that the metabolic basis for MP cell production of IFN-γ in response to TCR stimulation differs from that of effector T cells. MP cells used both mitochondrial and cytoplasmic metabolism and made use of glucose and glutamine to fuel sensitive IFN-γ responses to weak TCR agonism. In contrast, IFN-γ production by effector T cells was less responsive to weak TCR stimulation and required cytoplasmic glycolysis, while glutaminolysis and transport of pyruvate into the mitochondria were dispensable.

DISCUSSION

T cell reconstitution remains a central problem in patients who have undergone severe lymphopenia during clinical protocols such as hematopoietic transplantation or intensive chemotherapy, and in particular the $CD4^+$ T cell compartment is typically very slow to recover.[41,42] Homeostatic proliferation is a major mechanism driving the recovery of T cells in these settings.[23] Studies using murine models have established that IL-7-dependent slow homeostatic expansion maintains $CD4^+$ T cells in a naive state where they can provide a reservoir for subsequent responses to specific antigenic challenges, while MHC class II-dependent rapid homeostatic proliferation leads to the expansion of an MP population comprising cells with diverse antigen specificities.[15] Little is known about the role of this MP population in anti-tumor immunity, and in particular it is not clear how their diverse TCR specificities contribute. We show here that human MP cells have elevated responsiveness to weak TCR stimulation compared to either effector T cells or T cells that underwent slow homeostatic proliferation, and this is associated with heightened IFN-γ production against autologous or allogeneic transformed B cells. Thus, due to their greater TCR sensitivity, MP cells may be able to respond to tumor cells in an innate-like manner through recognition of self-antigens or comparatively low-affinity allo-antigens. The availability of MP cells that arise through homeostatic proliferation may therefore provide a key source of early IFN-γ that contributes to tumor immunosurveillance during immune reconstitution.

Our results also demonstrate that MP cells possess a distinctive metabolic profile. Consistent with prior studies, umbilical cord blood T cells that were exposed to IL-2 and IL-7 alone causing them to proliferate slowly but retain a naive phenotype appeared metabolically quite quiescent, while cord T cells that differentiated into effectors through anti-CD3/CD28 and ICAM-1 stimulation typically showed a marked shift toward a glycolytic metabolic profile (Figure 6B). In contrast, MP cells concordantly upregulated glycolysis and respiratory activity, indicating elevated mitochondrial metabolism (Figure 6B). It is now well established that T cells that receive strong TCR stimulation undergo extensive calcium signaling and that this leads to multiple changes in metabolic pathways including activation of both aerobic glycolysis and mitochondrial metabolism.[43] Effector T_{H1} cells ultimately shift toward a high dependence on aerobic glycolysis, which resembles a metabolic program first observed in cancer cells termed the Warburg effect.[44,45] In contrast, homeostatic activation pathways produce much weaker tonic TCR stimulation that mainly engages a subset of the downstream signaling molecules such as ERK and mTOR.[46,47] We found that MP cells showed highly efficient and rapid ERK phosphorylation in response to a low level of TCR stimulation and that they utilized both mitochondrial respiration and aerobic glycolysis for IFN-γ production. Phosphorylation of ERK has been shown to be critical in promoting mitochondrial oxidation of glutamine,[40] and glutaminolysis is now recognized for its importance in facilitating an effective T_{H1} immune response.[48] Moreover, several targets downstream of mTOR have been shown to regulate transcription factors and genes that play an important role in mitochondrial metabolic reprogramming and T cell function (reviewed by Myers et al.[49]). Thus, it is intriguing to speculate that the relatively weak TCR

stimulation encountered by MP cells, which induces little calcium signaling but activates ERK and mTOR pathways, avoids the extreme shift toward aerobic glycolysis of effector T cells and instead allows MP cells to maintain a metabolic phenotype that utilizes mitochondrial respiration to enable metabolism of additional substrates such as glutamine.

A key question is whether the metabolic phenotype of MP cells provides them with a functional advantage as anti-tumor effectors. While the importance of aerobic glycolysis in IFN-γ production by effector T cells is well established, a high dependence on glycolytic metabolism is also associated with exhaustion and poor anti-tumor function.[50] We hypothesize that the tonic TCR signaling received during MP differentiation preserves robust mitochondria. Based on prior work that highlights the importance of mitochondrial function in effective and long-lasting T cell-mediated tumor control,[51] MP cells may therefore be better able to mediate sustained anti-tumor responses compared to effector T cells that differentiate in response to strong antigenic stimulation. However, while this capacity could provide critical protection against cancer relapse, it remains unclear whether MP cells selectively target neoplastic cells. Our results are consistent with prior indications that MP cells have diverse antigen specificities[15] and that the responses we observed to B lymphoblastoid spheroids are mediated via weak TCR stimulation resulting from binding to self-MHC molecules or low-affinity alloreactivity. Whether MP cells also distinguish features specific to lymphoma cells such as the presence of tumor-associated antigens or stress ligands that allow them to selectively target neoplastic cells is not known. Since prior studies have implicated MP cells in immune-mediated pathologies,[11,12,14] it is also possible that they do not respond selectively to transformed cells and are simply highly prone to mediating auto- or alloreactive responses. Hence, a critical area of investigation for future studies will be to determine the role of MP cells in GVHD. Overall, our analysis suggests that, due to their high TCR sensitivity and distinctive metabolic profile, MP cells occupy a unique immunological niche that may provide key protective responses but that may also be susceptible to pathological outcomes.

Limitations of the study

A central limitation is that our studies were focused on MP cells derived from human umbilical cord blood that were differentiated *in vitro*. It will therefore be important to confirm in future studies that MP cells that differentiate *in vivo* have similar properties. Additionally, cord blood T cells are enriched for fetally derived subsets of T cells that may differ functionally from T cells that arise later in life. It will therefore be of interest in future studies to determine whether MP cells derived from adult progenitors are also characterized by the metabolic phenotype and high TCR sensitivity that we have identified, or whether this mode of T cell differentiation occurs mainly in neonatal T cell populations.

STAR★METHODS

Detailed methods are provided in the online version of this paper and include the following:

- KEY RESOURCES TABLE
- RESOURCE AVAILABILITY
  - Lead contact
  - Materials availability
  - Data and code availability
- EXPERIMENTAL MODEL AND STUDY PARTICIPANT DETAILS
  - Design of *in vitro* experiments
  - Human tissue samples
  - Design of xenotransplantation experiments
- METHOD DETAILS
  - Cellular isolation
  - Flow cytometric analysis
  - Homeostatic differentiation *in vitro*
  - Responses to secondary stimulation
  - Metabolic analyses
- QUANTIFICATION AND STATISTICAL ANALYSIS

SUPPLEMENTAL INFORMATION

Supplemental information can be found online at https://doi.org/10.1016/j.isci.2024.109775.

ACKNOWLEDGMENTS

Major support was provided by NIH R01 AI136500 (J.E.G.); additional support was provided by the University of Wisconsin-Madison's Office of the Vice Chancellor for Research and Graduate Education Fall Research Competition Program.

Collection of cord blood was supported in part by the Human Subjects Core of the Department of Obstetrics and Gynecology at UW-Madison.

The authors thank Boehringer-Ingelheim for generously providing BI-1950 (LFA-1 antagonist) and BI-9446 (negative control) compounds.

AUTHOR CONTRIBUTIONS

Conceptualization: N.S.B., N.A.Z., and J.E.G. Data curation and formal analysis: N.S.B. Methodology: N.S.B., N.A.Z., A.K., M.P., and J.E.G. Investigation: N.S.B. and N.A.Z. Visualization: N.S.B. and J.E.G. Funding acquisition: J.E.G. Project administration: J.E.G. Resources: M.P. Supervision: M.P. and J.E.G. Validation: N.S.B. Visualization: N.S.B. and J.E.G. Writing – original draft: N.S.B. Writing – review and editing: J.E.G.

DECLARATION OF INTERESTS

J.E.G. is a member of the Scientific Advisory Board of MiNK Therapeutics and was the recipient of a Sponsored Research Award from Shattuck Laboratories; neither MiNK Therapeutics nor Shattuck Laboratories played any part in the design, conduct, analysis, or interpretation of the studies reported here.

A.K. is an employee of Qiagen Sciences, Inc; Qiagen Sciences played no part in the design, conduct, analysis, or interpretation of the studies reported here.

Received: January 10, 2024
Revised: March 12, 2024
Accepted: April 15, 2024
Published: April 18, 2024

REFERENCES

1. Wang, H., and Yang, Y.G. (2014). The complex and central role of interferon-gamma in graft-versus-host disease and graft-versus-tumor activity. Immunol. Rev. *258*, 30–44. https://doi.org/10.1111/imr.12151.
2. Ricciardi, S., Manfrini, N., Alfieri, R., Calamita, P., Crosti, M.C., Gallo, S., Müller, R., Pagani, M., Abrignani, S., and Biffo, S. (2018). The Translational Machinery of Human CD4(+) T Cells Is Poised for Activation and Controls the Switch from Quiescence to Metabolic Remodeling. Cell Metab. *28*, 895–906.e5. https://doi.org/10.1016/j.cmet.2018.08.009.
3. Komori, H.K., Hart, T., LaMere, S.A., Chew, P.V., and Salomon, D.R. (2015). Defining CD4 T cell memory by the epigenetic landscape of CpG DNA methylation. J. Immunol. *194*, 1565–1579. https://doi.org/10.4049/jimmunol.1401162.
4. Fox, C.J., Hammerman, P.S., and Thompson, C.B. (2005). Fuel feeds function: energy metabolism and the T-cell response. Nat. Rev. Immunol. *5*, 844–852. https://doi.org/10.1038/nri1710.
5. Zhu, J., Yamane, H., and Paul, W.E. (2010). Differentiation of effector CD4 T cell populations (*). Annu. Rev. Immunol. *28*, 445–489. https://doi.org/10.1146/annurev-immunol-030409-101212.
6. Gudmundsdottir, H., and Turka, L.A. (2001). A closer look at homeostatic proliferation of CD4+ T cells: costimulatory requirements and role in memory formation. J. Immunol. *167*, 3699–3707. https://doi.org/10.4049/jimmunol.167.7.3699.
7. Sprent, J., and Surh, C.D. (2011). Normal T cell homeostasis: the conversion of naive cells into memory-phenotype cells. Nat. Immunol. *12*, 478–484. https://doi.org/10.1038/ni.2018.
8. Kawabe, T., and Sher, A. (2022). Memory-phenotype CD4 + T cells: a naturally arising T lymphocyte population possessing innate immune function. Int. Immunol. *34*, 189–196. https://doi.org/10.1093/intimm/dxab108.
9. Su, L.F., Kidd, B.A., Han, A., Kotzin, J.J., and Davis, M.M. (2013). Virus-specific CD4(+) memory-phenotype T cells are abundant in unexposed adults. Immunity *38*, 373–383. https://doi.org/10.1016/j.immuni.2012.10.021.
10. Kawabe, T., Jankovic, D., Kawabe, S., Huang, Y., Lee, P.H., Yamane, H., Zhu, J., Sher, A., Germain, R.N., and Paul, W.E. (2017). Memory-phenotype CD4(+) T cells spontaneously generated under steady-state conditions exert innate TH1-like effector function. Sci. Immunol. *2*, eaam9304. https://doi.org/10.1126/sciimmunol.aam9304.
11. King, C., Ilic, A., Koelsch, K., and Sarvetnick, N. (2004). Homeostatic expansion of T cells during immune insufficiency generates autoimmunity. Cell *117*, 265–277. https://doi.org/10.1016/s0092-8674(04)00335-6.
12. Khiong, K., Murakami, M., Kitabayashi, C., Ueda, N., Sawa, S.I., Sakamoto, A., Kotzin, B.L., Rozzo, S.J., Ishihara, K., Verella-Garcia, M., et al. (2007). Homeostatically proliferating CD4 T cells are involved in the pathogenesis of an Omenn syndrome murine model. J. Clin. Invest. *117*, 1270–1281. https://doi.org/10.1172/JCI30513.
13. Moxham, V.F., Karegli, J., Phillips, R.E., Brown, K.L., Tapmeier, T.T., Hangartner, R., Sacks, S.H., and Wong, W. (2008). Homeostatic proliferation of lymphocytes results in augmented memory-like function and accelerated allograft rejection. J. Immunol. *180*, 3910–3918. https://doi.org/10.4049/jimmunol.180.6.3910.
14. Jones, J.L., Thompson, S.A.J., Loh, P., Davies, J.L., Tuohy, O.C., Curry, A.J., Azzopardi, L., Hill-Cawthorne, G., Fahey, M.T., Compston, A., and Coles, A.J. (2013). Human autoimmunity after lymphocyte depletion is caused by homeostatic T-cell proliferation. Proc. Natl. Acad. Sci. USA *110*, 20200–20205. https://doi.org/10.1073/pnas.1313654110.
15. Min, B., and Paul, W.E. (2005). Endogenous proliferation: burst-like CD4 T cell proliferation in lymphopenic settings. Semin. Immunol. *17*, 201–207. https://doi.org/10.1016/j.smim.2005.02.005.
16. Min, B. (2018). Spontaneous T Cell Proliferation: A Physiologic Process to Create and Maintain Homeostatic Balance and Diversity of the Immune System. Front. Immunol. *9*, 547. https://doi.org/10.3389/fimmu.2018.00547.
17. Le Campion, A., Bourgeois, C., Lambolez, F., Martin, B., Léaument, S., Dautigny, N., Tanchot, C., Pénit, C., and Lucas, B. (2002). Naive T cells proliferate strongly in neonatal mice in response to self-peptide/self-MHC complexes. Proc. Natl. Acad. Sci. USA *99*, 4538–4543. https://doi.org/10.1073/pnas.062621699.
18. Kieper, W.C., Troy, A., Burghardt, J.T., Ramsey, C., Lee, J.Y., Jiang, H.Q., Dummer, W., Shen, H., Cebra, J.J., and Surh, C.D. (2005). Recent immune status determines the source of antigens that drive homeostatic T cell expansion. J. Immunol. *174*, 3158–3163. https://doi.org/10.4049/jimmunol.174.6.3158.
19. Min, B., Yamane, H., Hu-Li, J., and Paul, W.E. (2005). Spontaneous and homeostatic proliferation of CD4 T cells are regulated by different mechanisms. J. Immunol. *174*, 6039–6044. https://doi.org/10.4049/jimmunol.174.10.6039.
20. Do, J.S., and Min, B. (2009). Differential requirements of MHC and of DCs for endogenous proliferation of different T-cell subsets *in vivo*. Proc. Natl. Acad. Sci. USA *106*, 20394–20398. https://doi.org/10.1073/pnas.0909954106.
21. Onoe, T., Kalscheuer, H., Chittenden, M., Zhao, G., Yang, Y.G., and Sykes, M. (2010). Homeostatic expansion and phenotypic conversion of human T cells depend on peripheral interactions with APCs. J. Immunol. *184*, 6756–6765. https://doi.org/10.4049/jimmunol.0901711.
22. Kawabe, T., Sun, S.L., Fujita, T., Yamaki, S., Asao, A., Takahashi, T., So, T., and Ishii, N. (2013). Homeostatic proliferation of naive CD4+ T cells in mesenteric lymph nodes generates gut-tropic Th17 cells. J. Immunol. *190*, 5788–5798. https://doi.org/10.4049/jimmunol.1203111.
23. Tchao, N.K., and Turka, L.A. (2012). Lymphodepletion and homeostatic proliferation: implications for transplantation. Am. J. Transplant. *12*, 1079–1090. https://doi.org/10.1111/j.1600-6143.2012.04008.x.
24. Peng, M., Yin, N., Chhangawala, S., Xu, K., Leslie, C.S., and Li, M.O. (2016). Aerobic glycolysis promotes T helper 1 cell

differentiation through an epigenetic mechanism. Science *354*, 481–484. https://doi.org/10.1126/science.aaf6284.

25. Chang, C.H., Curtis, J.D., Maggi, L.B., Jr., Faubert, B., Villarino, A.V., O'Sullivan, D., Huang, S.C.C., van der Windt, G.J.W., Blagih, J., Qiu, J., et al. (2013). Posttranscriptional control of T cell effector function by aerobic glycolysis. Cell *153*, 1239–1251. https://doi.org/10.1016/j.cell.2013.05.016.
26. Menk, A.V., Scharping, N.E., Moreci, R.S., Zeng, X., Guy, C., Salvatore, S., Bae, H., Xie, J., Young, H.A., Wendell, S.G., and Delgoffe, G.M. (2018). Early TCR Signaling Induces Rapid Aerobic Glycolysis Enabling Distinct Acute T Cell Effector Functions. Cell Rep. *22*, 1509–1521. https://doi.org/10.1016/j.celrep.2018.01.040.
27. Snook, J.P., Kim, C., and Williams, M.A. (2018). TCR signal strength controls the differentiation of CD4(+) effector and memory T cells. Sci. Immunol. *3*, eaas9103. https://doi.org/10.1126/sciimmunol.aas9103.
28. Kohler, S., and Thiel, A. (2009). Life after the thymus: CD31+ and CD31- human naive CD4+ T-cell subsets. Blood *113*, 769–774. https://doi.org/10.1182/blood-2008-02-139154.
29. Haines, C.J., Giffon, T.D., Lu, L.S., Lu, X., Tessier-Lavigne, M., Ross, D.T., and Lewis, D.B. (2009). Human CD4+ T cell recent thymic emigrants are identified by protein tyrosine kinase 7 and have reduced immune function. J. Exp. Med. *206*, 275–285. https://doi.org/10.1084/jem.20080996.
30. Jacks, R.D., Keller, T.J., Nelson, A., Nishimura, M.I., White, P., and Iwashima, M. (2018). Cell intrinsic characteristics of human cord blood naive CD4T cells. Immunol. Lett. *193*, 51–57. https://doi.org/10.1016/j.imlet.2017.11.011.
31. Chen, L., Cohen, A.C., and Lewis, D.B. (2006). Impaired allogeneic activation and T-helper 1 differentiation of human cord blood naive CD4 T cells. Biol. Blood Marrow Transplant. *12*, 160–171. https://doi.org/10.1016/j.bbmt.2005.10.027.
32. Hess, N.J., Hudson, A.W., Hematti, P., and Gumperz, J.E. (2020). Early T Cell Activation Metrics Predict Graft-versus-Host Disease in a Humanized Mouse Model of Hematopoietic Stem Cell Transplantation. J. Immunol. *205*, 272–281. https://doi.org/10.4049/jimmunol.2000054.
33. Hess, N.J., N, S.B., Bobeck, E.A., McDougal, C.E., Ma, S., Sauer, J.D., Hudson, A.W., and Gumperz, J.E. (2021). iNKT cells coordinate immune pathways to enable engraftment in nonconditioned hosts. Life Sci. Alliance *4*, e202000999. https://doi.org/10.26508/lsa.202000999.
34. Zumwalde, N.A., Sharma, A., Xu, X., Ma, S., Schneider, C.L., Romero-Masters, J.C., Hudson, A.W., Gendron-Fitzpatrick, A., Kenney, S.C., and Gumperz, J.E. (2017). Adoptively transferred Vgamma9Vdelta2 T cells show potent antitumor effects in a preclinical B cell lymphomagenesis model. JCI Insight *2*, e93179. https://doi.org/10.1172/jci.insight.93179.
35. Afkarian, M., Sedy, J.R., Yang, J., Jacobson, N.G., Cereb, N., Yang, S.Y., Murphy, T.L., and Murphy, K.M. (2002). T-bet is a STAT1-induced regulator of IL-12R expression in naive CD4+ T cells. Nat. Immunol. *3*, 549–557. https://doi.org/10.1038/ni794.
36. Szabo, S.J., Kim, S.T., Costa, G.L., Zhang, X., Fathman, C.G., and Glimcher, L.H. (2000). A novel transcription factor, T-bet, directs Th1 lineage commitment. Cell *100*, 655–669. https://doi.org/10.1016/s0092-8674(00)80702-3.
37. Bird, J.J., Brown, D.R., Mullen, A.C., Moskowitz, N.H., Mahowald, M.A., Sider, J.R., Gajewski, T.F., Wang, C.R., and Reiner, S.L. (1998). Helper T cell differentiation is controlled by the cell cycle. Immunity *9*, 229–237. https://doi.org/10.1016/s1074-7613(00)80605-6.
38. Reiner, S.L., Mullen, A.C., Hutchins, A.S., and Pearce, E.L. (2003). Helper T cell differentiation and the problem of cellular inheritance. Immunol. Res. *27*, 463–468. IR:27:2-3:463 [pii]10.1385/IR:27:2-3:463.
39. Rogers, P.R., Grey, H.M., and Croft, M. (1998). Modulation of naive CD4 T cell activation with altered peptide ligands: the nature of the peptide and presentation in the context of costimulation are critical for a sustained response. J. Immunol. *160*, 3698–3704.
40. Carr, E.L., Kelman, A., Wu, G.S., Gopaul, R., Senkevitch, E., Aghvanyan, A., Turay, A.M., and Frauwirth, K.A. (2010). Glutamine uptake and metabolism are coordinately regulated by ERK/MAPK during T lymphocyte activation. J. Immunol. *185*, 1037–1044. https://doi.org/10.4049/jimmunol.0903586.
41. Storek, J., Witherspoon, R.P., and Storb, R. (1995). T cell reconstitution after bone marrow transplantation into adult patients does not resemble T cell development in early life. Bone Marrow Transplant. *16*, 413–425.
42. Mackall, C.L., Fleisher, T.A., Brown, M.R., Andrich, M.P., Chen, C.C., Feuerstein, I.M., Magrath, I.T., Wexler, L.H., Dimitrov, D.S., and Gress, R.E. (1997). Distinctions between CD8+ and CD4+ T-cell regenerative pathways result in prolonged T-cell subset imbalance after intensive chemotherapy. Blood *89*, 3700–3707.
43. Wang, Y., Tao, A., Vaeth, M., and Feske, S. (2020). Calcium regulation of T cell metabolism. Curr. Opin. Physiol. *17*, 207–223. https://doi.org/10.1016/j.cophys.2020.07.016.
44. Pearce, E.L., and Pearce, E.J. (2013). Metabolic pathways in immune cell activation and quiescence. Immunity *38*, 633–643. https://doi.org/10.1016/j.immuni.2013.04.005.
45. Guo, C., Chen, S., Liu, W., Ma, Y., Li, J., Fisher, P.B., Fang, X., and Wang, X.Y. (2019). Immunometabolism: A new target for improving cancer immunotherapy. Adv. Cancer Res. *143*, 195–253. https://doi.org/10.1016/bs.acr.2019.03.004.
46. Stefanová, I., Hemmer, B., Vergelli, M., Martin, R., Biddison, W.E., and Germain, R.N. (2003). TCR ligand discrimination is enforced by competing ERK positive and SHP-1 negative feedback pathways. Nat. Immunol. *4*, 248–254.
47. Myers, D.R., Norlin, E., Vercoulen, Y., and Roose, J.P. (2019). Active Tonic mTORC1 Signals Shape Baseline Translation in Naive T Cells. Cell Rep. *27*, 1858–1874.e6. https://doi.org/10.1016/j.celrep.2019.04.037.
48. Klysz, D., Tai, X., Robert, P.A., Craveiro, M., Cretenet, G., Oburoglu, L., Mongellaz, C., Floess, S., Fritz, V., Matias, M.I., et al. (2015). Glutamine-dependent alpha-ketoglutarate production regulates the balance between T helper 1 cell and regulatory T cell generation. Sci. Signal. *8*, ra97. https://doi.org/10.1126/scisignal.aab2610.
49. Myers, D.R., Wheeler, B., and Roose, J.P. (2019). mTOR and other effector kinase signals that impact T cell function and activity. Immunol. Rev. *291*, 134–153. https://doi.org/10.1111/imr.12796.
50. Buck, M.D., O'Sullivan, D., Klein Geltink, R.I., Curtis, J.D., Chang, C.H., Sanin, D.E., Qiu, J., Kretz, O., Braas, D., van der Windt, G.J.W., et al. (2016). Mitochondrial Dynamics Controls T Cell Fate through Metabolic Programming. Cell *166*, 63–76. https://doi.org/10.1016/j.cell.2016.05.035.
51. van der Windt, G.J.W., O'Sullivan, D., Everts, B., Huang, S.C.C., Buck, M.D., Curtis, J.D., Chang, C.H., Smith, A.M., Ai, T., Faubert, B., et al. (2013). CD8 memory T cells have a bioenergetic advantage that underlies their rapid recall ability. Proc. Natl. Acad. Sci. USA *110*, 14336–14341. https://doi.org/10.1073/pnas.1221740110.

STAR★METHODS

KEY RESOURCES TABLE

REAGENT or RESOURCE	SOURCE	IDENTIFIER
Antibodies		
anti-human CD3 (HIT3a)	Biolegend	Cat# 300324; RRID:AB_493738
anti-human CD4 (OKT4)	Biolegend	Cat# 317408; RRID:AB_571950
anti-human CD8 (HIT8a)	Biolegend	Cat# 344750; RRID:AB_2044008
anti-human CD14 (63D3)	Biolegend	Cat# 367108; RRID:AB_2566710
anti-human CD45 (HI30)	Biolegend	Cat# 304036; RRID:AB_2561383
anti-human HLA-A,B,C (W6/32)	Biolegend	Cat# 311438; RRID:AB_2566306
anti-human CD45RO (UCHL1)	Biolegend	Cat# 304242; RRID:AB_314420
anti-human CD45RA (HI100)	Biolegend	Cat# 304122; RRID:AB_893357
anti-human CD31 (WM59)	Biolegend	Cat# 303116; RRID:AB_1877151
anti-human CD69 (FN50)	Biolegend	Cat# 310912; RRID:AB_314847
anti-human IL-8 (BH0814)	Biolegend	Cat# 511406; RRID:AB_893462
anti-human IFN−γ (4S.B3)	Biolegend	Cat# 502506; RRID:AB_315230
anti-human IL-4 (8D4-8)	Biolegend	Cat# 500712; RRID:AB_1877137
anti-human IL-13 (JES10-5A2)	Biolegend	Cat# 501911; RRID:AB_2124283
anti-human IL-17A (N49-653)	Biolegend	Cat# 512312; RRID:AB_961392
anti-human IL-10 (JES3-9D7)	Biolegend	Cat# 501404; RRID:AB_315170
anti-human IL-2 (MQ1-17H12)	Biolegend	Cat# 500324; RRID:AB_2125595
anti-human TNF-α (Mab11)	Biolegend	Cat# 502930; RRID:AB_2204079
anti-human FoxP3 (259D)	Biolegend	Cat# 320114; RRID:AB_439754
anti-human phospho-ERK (6B8B69)	Biolegend	Cat# 369506; RRID:AB_2629705
anti-human phospho-ZAP-70 (A16043E)	Biolegend	Cat# 396004; RRID:AB_2801068
anti-human T-bet (04-46)	BD Biosciences	Cat# 561268; RRID:AB_10564071
anti-human CD212 or IL-12Rβ2 (2B6/ 12beta2)	BD Biosciences	Cat# 550723; RRID:AB_393851
Cell Trace Violet	Thermo Fisher Scientific	Cat# C34557
JC-10 Kit	Biolegend	Cat# 421902
MitoTrackerGreen	Thermo Fisher Scientific	Cat#M7514
MitoTracker™ Red CMXRos	Thermo Fisher Scientific	Cat# M7512
Biological samples		
Human umbilical cord blood	Neonates	N/A
Human adult peripheral blood	Healthy adults	N/A
Chemicals, peptides, and recombinant proteins		
Recombinant Human IL-2	Peprotech	Cat# 200-02
Recombinant Human IL-7	Peprotech	Cat# 200-07
BI-1950 (LFA-1 antagonist) and BI-9446 (Negative control compound)	Boehringer-Ingelheim	https://www.opnme.com/molecules/lfa-1-bi-1950
anti-CD54 blocking mAb	Biolegend	Cat# 322722
anti-MHC class II (Tu39 or L243) blocking mAb	BD Biosciences or purified from hybridoma supernatants	Cat# 555557
ImmunoCult™ Human CD3/CD28 T cell Activator	Stemcell Technologies	Cat# 10971
Purified anti-human CD3 Antibody (OKT3)	Biolegend	Cat# 317326
Purified anti-human CD28 Antibody (CD28.2)	Biolegend	Cat# 302923

(*Continued on next page*)

Continued

REAGENT or RESOURCE	SOURCE	IDENTIFIER
Human ICAM-1 Fc fusion protein	Acro Biosystems	Cat# IC1-H5250
2-deoxy-D−γlucose (2-DG)	Thermo Scientific	Cat# 111980050
UK 5099	Millipore Sigma	Cat# PZ0160
Bis-2-(5-phenylacetamido-1,3,4-thiadiazol-2-yl) ethyl sulfide (BPTES)	Millipore Sigma	Cat# SML0601
Etomoxir	Cayman Chemical	Cat# NC1003732
Galloflavin	Cayman Chemical	Cat# NC1176296
Oligomycin	Millipore Sigma	Cat# 49545510MG
Cell Activation Cocktail with Brefeldin A	Biolegend	Cat# 423304
Poly-L-Lysine	Advanced biomatrix	Cat# 5048
Precision Count Beads	Biolegend	Cat# 424902
Cyto-Fast Fix/Perm buffer Set	Biolegend	Cat# 426803
Transcription factor Buffer Set	BD Biosciences	Cat# 565575
Transcription factor Buffer Set	BD Biosciences	Cat# 565575
True-Phos™ Perm Buffer Set	Biolegend	Cat# 425401
Critical commercial assays		
ATP Assay Kit	Abcam	Cat# ab83355
Seahorse XF Cell Energy Phenotype Test Kit	Agilent	Cat# 103325-100
Experimental models: Organisms/strains		
NOD/SCID/$\gamma_c^{-/-}$ (NSG) mice, Strain #:005557	Jackson Labs	RRID:IMSR_JAX:005557
Epstein-Barr virus, M81 strain	Culture supernatants of stably infected cells	N/A
Software and algorithms		
FlowJo	Treestar	https://www.flowjo.com/
Graphpad Prism 9	Graphpad	https://www.graphpad.com/scientificsoftware/prism/
Seahorse Wave Desktop Software	Agilent	https://www.agilent.com
Other		
Cell culture medium: RPMI 1640 (standard)	Corning	Cat# 10040CV
Cell culture medium: RPMI 1640 (no glucose, no glutamine)	Biological Industries	Cat# 01-101-1A

RESOURCE AVAILABILITY

Lead contact

Further information and requests for resources and reagents should be directed to and will be fulfilled by the lead contact, Jenny Gumperz (jegumperz@wisc.edu).

Materials availability

This study did not generate new unique reagents.

Data and code availability

- [All] data reported in this paper will be shared by the lead contact upon request.
- This paper does not report original code.
- Any additional information required to reanalyze the data reported in this paper is available from the lead contact upon request.

EXPERIMENTAL MODEL AND STUDY PARTICIPANT DETAILS

Design of *in vitro* experiments

For each experiment, $CD4^+$ T cells were isolated from a primary human umbilical cord blood sample, and cells from the same sample were exposed in parallel to the indicated culture conditions (see method details for information on conditions). Experiments were repeated multiple times using unrelated cord blood samples, and results from like treatment conditions were aggregated for data analysis.

Human tissue samples

Human umbilical cord blood samples were collected at birth with informed consent and obtained under UW-Madison Minimal Risk IRB Not Human Subjects Research Exemptions 2017-0870 and 2023-0392. As specified in these protocols, de-identified samples were provided without any accompanying information (e.g. sex, race, gender, ancestry, socioeconomic status) from the following institutions: the Obstetrics and Gynecology department at Meriter Hospital, Madison, WI; the Cleveland Cord Blood Center; the UC Davis Health California Cord Blood Collection Program; or the Carolinas Cord Blood Bank. Peripheral blood samples used in this study were acquired from healthy adult subjects (i.e. 18 years or older) with informed consent under UW-Madison Minimal Risk IRB protocol 2018-0304. Subjects were not included or excluded on the basis of age, sex/gender, ancestry, race, ethnicity, or socioeconomic status. In accordance with this IRB protocol, providing data regarding sex and race was optional, and no other personal information (e.g. gender, ancestry, socioeconomic status) was collected.

Design of xenotransplantation experiments

Animal studies were performed in accordance with UW-Madison IACUC protocol M005199. Immunodeficient NOD/SCID/$\gamma_c^{-/-}$ (NSG) mice were purchased from Jackson Laboratories and bred and maintained in specific pathogen free facilities using aseptic housing. Male and female mice 6-12 weeks of age were used for experiments. Primary human cord blood mononuclear cells (CBMCs) were injected intravenously at a dose of at 1×10^7 cells per mouse. For analysis of T cells from EBV-infected vs. uninfected conditions, CBMCs were exposed to 2,000 U of the M81 strain of EBV or mock treated in medium alone for 2 hours, then administered intraperitoneally at 1×10^7 cells per mouse. Experiments included 3-5 mice per group, and were not performed in a blinded manner. Mice were caged according to sex and approximately equivalent numbers of males and females were used in each experiment. Mice were euthanized at indicated timepoints and cells collected from spleen tissue for analysis. Two exclusion criteria were set *a priori*: *i*) mice that died prior to the pre-determined endpoint; *ii*) mice that were found not to contain any detectable human cells in the spleen. The first exclusion criterion was not met in any of the experiments, while one mouse met the second criterion in one of the experiments (Figure 2A).

METHOD DETAILS

Cellular isolation

Mononuclear cells were isolated by density gradient centrifugation using Ficoll-plaque PLUS (GE Healthcare). $CD14^+$ monocytes were positively isolated using magnetic beads (Miltenyi Biotec). $CD4^+$ T cells were magnetically isolated by positive selection using anti-CD4 beads, or by negative selection using a CD4 T cell isolation kit (Miltenyi Biotec) or EasySep CD4 T cell isolation kit (Stemcell technologies). To isolate $CD31^+$ and CD31- subsets, isolated CD4 T cells were indirectly labelled with PE conjugated anti-CD31 antibody and sorted using anti-PE magnetic beads.

Flow cytometric analysis

Cells were resuspended in phosphate buffered saline (PBS) containing 5% bovine calf serum (BCS), 20% human AB serum and 0.1% sodium azide, then labeled with fluorescent antibodies for 20 min at 4°C. For intracellular analyses, T cells were stimulated with PMA/ionomycin in the presence of brefeldin A for 4h, then fixed and permeabilized (Cyto-Fast Fix/Perm buffer set, Biolegend) prior to staining. Transcription factor staining was performed according to the manufacturer's protocol using BD Biosciences' transcription factor buffer set. Analysis of phospho-ERK and phospho-ZAP-70 was performed using True-Phos Perm buffer set (Biolegend). For MitoTrackerRed staining, T cells were incubated in pre-warmed RPMI culture medium containing 50nM MitoTracker Red dye for 30 min at 37°C. Cells were washed and resuspended in fresh warm culture medium and read immediately by flow cytometry.

For analysis of intracellular cytokines produced by human T cells from xenotransplanted mice, splenocytes were harvested at the indicated time points, then stimulated using PMA/ionomycin in the presence of brefeldin A (Biolegend) for 4h, then stained for cell surface markers to allow identification of human cells (CD45, HLA, CD3, CD4, CD8) prior to fixation and permabilization and staining for cytokines or negative control antibodies. Expansion of transplanted $CD4^+$ and $CD8^+$ T cells was quantified by assessing the total number of each human cell type in the spleen at the indicated time points using counting beads.

Homeostatic differentiation *in vitro*

$CD4^+$ T cells purified from cord blood were cultured at 37°C and 5% CO_2 in medium consisting of RPMI 1640, 10% BCS (Hyclone), 5% fetal bovine serum (FBS) (Hyclone or Gibco), 3% pooled human AB serum (Gemini), 1% Penicillin/Streptomycin, 1% L−Glutamine, 50 U/ml recombinant human IL-2 and 1 ng/ml recombinant human IL-7 (Peprotech). To generate effector T cells, $CD4^+$ cord T cells (5×10^4/well) were cultured in the presence of 2 μg/ml plate-bound anti-CD3 mAb, 2 μg/ml plate-bound recombinant human ICAM-1 Fc fusion protein (Acro

Biosystems), and 4 μg/ml soluble anti-CD28 mAb. MP cells were generated by co-culturing $CD4^+$ cord T cells at a 2:1 ratio with autologous monocytes. T cells were removed from the stimulation wells after 3-5 days (timing was chosen to provide a consistent amount of proliferation across experiments) and placed into wells containing IL-2/IL-7 medium alone for an additional 5-7 days before using them for further analysis. For blocking experiments, 10 μg/ml anti-MHC class II, anti-ICAM-1, IgG_1 control mAb, or IgG_{2a} control mAb were added at the start of the co-culture with autologous monocytes. Alternatively, to block ICAM-LFA interactions, a small molecule antagonist of LFA-1 called BI-1950, or a chemically similar negative control compound called BI-9446 (both a generous gift from Boehringer-Ingelheim), were included in the co-cultures at a final concentration of 8 μg/ml.

Responses to secondary stimulation

LCLs generated from cord blood B cells were used to assess T cell responses to neoplastically transformed cells. LCLs were generated by incubating 1×10^6 CD14- and CD4-depleted CBMCs with 2,000 U of the M81 strain of EBV, and culturing the cells for 3-4 weeks in (RPMI 1640, 10% BCS, 1% Penicillin/Streptomycin and 1% L−γlutamine) at 37°C and 5% CO_2. For analysis of T cell responses, T cells were mixed at a 1:1 ratio with autologous or allogeneic LCLs, or with allogeneic LCLs in the presence of 2 μg/ml Staphylococcus enterotoxin C (a generous gift of Dr. Wilmara Salgado-Pabon), or incubated with titrated doses of human CD3/CD28 antibody complex (ImmunoCult™, Stemcell Technologies). After 24-48h stimulation, culture supernatants were harvested and secreted IFN−γ was quantitated by ELISA (Biolegend). Analyses of T cell IFN-γ production in the presence of restricted amounts of glucose or glutamine were carried out using culture medium made with dialyzed serum and using RPMI medium lacking both glucose and glutamine, to which glucose or glutamine were added to generate the indicated final concentrations. Where indicated T cell stimulation was performed in the presence of 10 mM 2-deoxy-D−glucose (2-DG), or 50-100 μM galloflavin, or 35 μM UK5099, or 12.5 μM BPTES, or 2.5 μM etomoxir, or 1uM oligomycin.

Metabolic analyses

Analyses of oxygen consumption rate (OCR) and extracellular acidification rate (ECAR) were performed using a Seahorse XF Analyzer (Agilent). T cells were placed at 2.5×10^5 cells/well into Seahorse culture plates that were pre-coated with 50 μg/ml Poly-L-Lysine (Advanced biomatrix). Where indicated, 1 μM each of oligomycin and carbonyl cyanide p-trifluoromethoxy-phenylhydrazone (FCCP) were added to induce maximal stress. JC-10 staining was performed according to the manufacturer's instructions. For MitoTracker Red and MitoTracker Green analyses, $5x10^5$ T cells were labelled at final concentrations of 50nM and 100nM, respectively. Cells were washed and analyzed by flow cytometry, or were imaged at multiple focal planes along the depth of the cell using a confocal microscope with a 63X oil immersion objective. Images were processed using Zeiss Zen software to generate orthogonal projection. Orthogonal projections of the images were converted to binary 8 bit images. Automatic image thresholding was used to set masks based on DAPI and MitoTracker fluorescence. Pixel area of masked particles were calculated and total MitoTracker area was normalized by total DAPI area for each image. T cell intracellular ATP concentrations were measured using a colorimetric assay (Abcam).

QUANTIFICATION AND STATISTICAL ANALYSIS

Two-tailed parametric paired t-tests were used to analyze datasets involving 4 or more independent cord samples, where cells from each sample were subjected to different treatment conditions in parallel. In cases involving less than 4 samples, data were analyzed using a two-tailed unpaired t-test. Mann-Whitney t-tests were used for comparisons between unrelated samples. Data involving analysis of the amount of inhibition compared to a mock-treated control were analyzed using a to-tailed one-sample t-test. * indicates $P \leq 0.05$; ** indicates $P \leq 0.01$; *** indicates $P \leq 0.001$.